# Location of the boundary between the metamorphic Southalpine basement and the Paleozoic sequences of the Carnic Alps : illite "crystallinity" and vitrinite reflectance data

Autor(en): **Sassi, Raffaele / Árkai, Péter / Lantai, Csaba**

Objekttyp: **Article**

Zeitschrift: **Schweizerische mineralogische und petrographische Mitteilungen = Bulletin suisse de minéralogie et pétrographie**

Band (Jahr): **75 (1995)**

Heft 3

PDF erstellt am: **10.06.2024**

Persistenter Link: https://doi.org/10.5169/seals-57164

*SCHWEIZ. MINERAL. PETROGR. MITT. 75, 399–412, 1995*

# Location of the boundary between the metamorphic Southalpine basement and the Paleozoic sequences of the Carnic Alps: illite "crystallinity" and vitrinite reflectance data

by *Raffaele Sassi*[1], *Péter Árkai*[2], *Csaba Lantai*[2] and *Corrado Venturini*[3]

**Abstract**

The Southalpine basement of the Eastern Alps consists of unmetamorphosed Paleozoic sequences in its easternmost part (Paleocarnic Chain) and greenschist facies metamorphic rocks (Metamorphic Southalpine Basement = MSB) elsewhere. Many authors tried to localize the boundary between the metamorphic and non-metamorphic domains. Recent studies demonstrated, by means of illite "crystallinity" data, that the locations of this boundary given in the maps are uncorrect; the boundary should occur more eastwards.

In order to ascertain the position of this boundary, illite "crystallinity" and vitrinite reflectance data have been used. Furthermore, measurements of $d_{33\bar{1},060}$ spacing of potassic white mica have been used for monitoring the pressure character of metamorphism. Nine sites were selected following structural criteria, and ca. 30 rock samples were collected in each site, making up a population of 256 rock samples of pelitic to silty composition.

As a consequence of the analytical results and their interpretation, the problem of the boundary location between the MSB and the "non-metamorphic" Paleocarnic Chain may be considered as solved. This boundary turns out to be located along the Val Bordaglia Line and has a tectonic character. Three further main considerations can be stressed: (i) the extension of the MSB is significantly larger than previously supposed; (ii) the previously assumed "non-metamorphic" sequences in Carnia are partly anchimetamorphic indeed; (iii) they include some tectonic slices of epimetamorphic grade.

*Keywords:* metamorphic Southalpine Basement, Paleocarnic Chain, Variscan anchimetamorphism, illite "crystallinity", vitrinite reflectance.

**Zusammenfassung**

Das südalpine Kristallin der Ostalpen besteht im östlichsten Teil (Paläokarnische Kette) aus nichtmetamorphen paläozoischen Sequenzen, während es im restlichen Bereich aus grünschieferfaziellen Gesteinen (MSB) aufgebaut wird. Die Grenze zwischen nichtmetamorphem- und metamorphem Basement wurde von zahlreichen Autoren versuchsweise gezogen. Neuere IC-Studien zeigen aber, dass die in den Karten dargestellte Grenze unkorrekt ist und weiter nach Osten verlegt werden muss.

Die Grenze zwischen nichtmetamorphem bzw. metamorphem Basement wurden mittels Illit-Kristallinitäts- und Vitrinit-Reflexionsdaten ermittelt. Zur Charakterisierung der Druckbedingungen wurden an Kali-Hellglimmer die $d_{33\bar{1},060}$-Gitterabstände gemessen. Neun Lokalitäten wurden nach strukturellen Kriterien zur Probennahme bestimmt. Pro Lokalität wurden etwa 30 Proben entnommen, so dass insgesamt eine Population von 256 pelitischen bis siltitischen Proben zur Auswertung herangezogen werden konnte.

Unseres Erachtens kann aufgrund der analytischen Daten und deren Interpretation die Problematik zur Lokalisierung der Grenze zwischen MSB und der "nichtmetamorphen" Paläokarnischen Kette als gelöst betrachtet werden. Diese Grenze folgt der Val-Bordaglia-Linie und hat tektonischen Charakter. Drei weitere wesentliche Punkte müssen hervorgehoben werden: (i) die Ausdehnung von MSB ist bedeutend grösser als bisher angenommen; (ii) die ursprünglich als nichtmetamorph erachteten Sequenzen Karniens sind tatsächlich teilweise anchimetamorph geprägt; (iii) einige tektonische Späne epizonaler Metamorphite sind in letzteren eingeschlossen.

[1] Department of Mineralogy and Petrology, University of Padova, C.so Garibaldi 37, I-35137 Padova, Italy.
[2] Laboratory for Geochemical Research, Hungarian Academy of Sciences, H-1112, Budapest, Budaörsi út 45, Hungary.
[3] Department of Earth Sciences, University of Pisa, via S. Maria 53, I-56126 Pisa, Italy.

## Introduction

In the Southalpine basement of the Eastern Alps, unmetamorphosed Paleozoic sequences occur in Carnia while greenschist facies metamorphic rocks outcrop in Pusteria. Many authors *(e.g. Metamorphic map of the Alps, 1973; Structural Model of Italy and Gravity map, 1990)* localized the boundary between the metamorphic and non-metamorphic domains as shown in figure 1. However, recent studies (ÁRKAI et al., 1991) demonstrated, by means of illite "crystallinity" (IC) data, that this location is uncorrect, and that the boundary should occur more eastwards.

The aim of the present work is to locate exactly this boundary. For this purpose, the thermometric methods based on illite "crystallinity" and vitrinite reflectance have been used.

## Geological setting

The Metamorphic Southalpine Basement (MSB for short) of the Eastern Alps outcrops, underneath the Upper Carboniferous to Mesozoic and Tertiary stratigraphic cover, in three main areas (inset of Fig. 1): (i) a northern, approximately west–est trending belt, from the Sarentino Valley

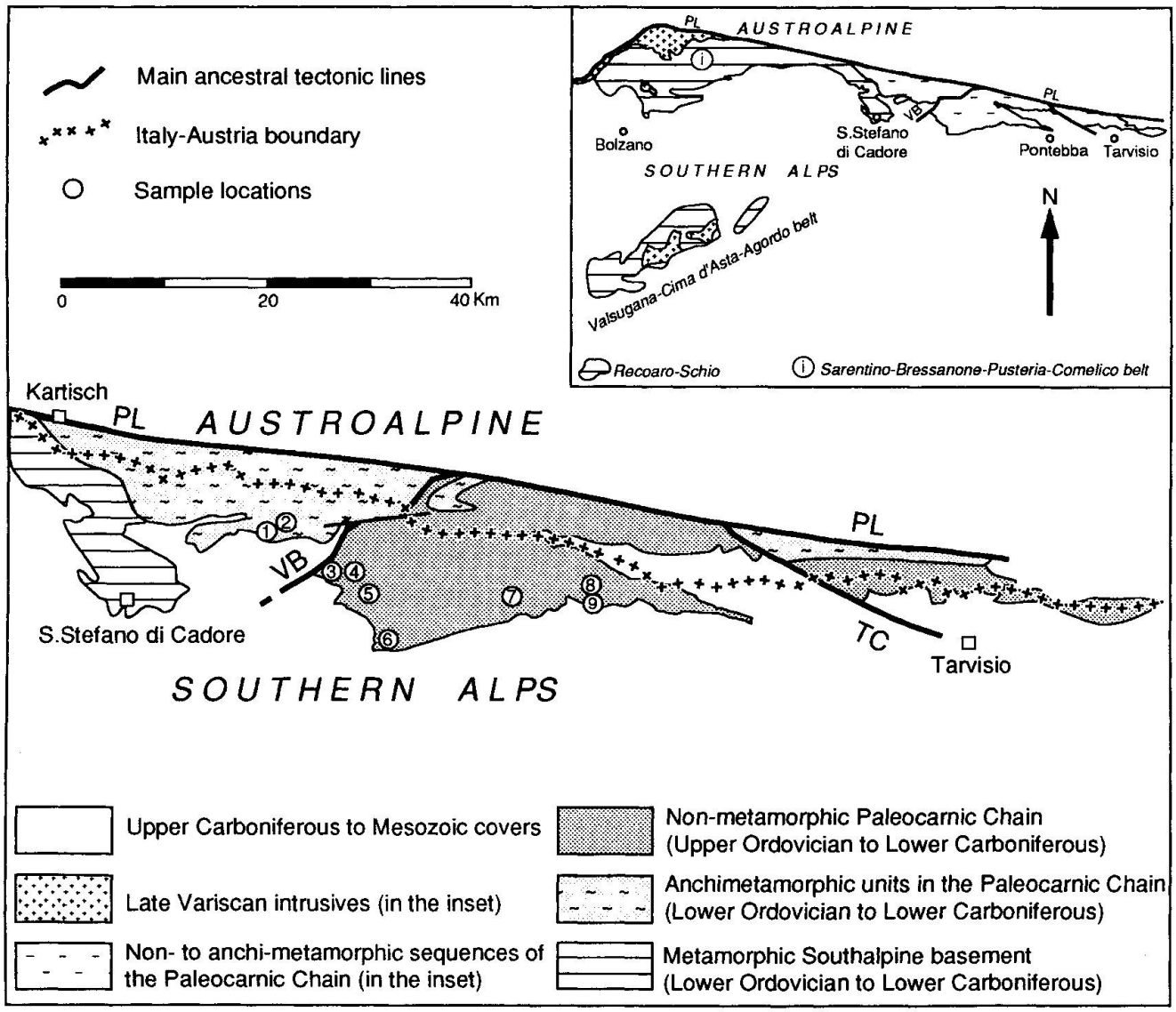


*Fig. 1* Location of the samples. The geological sketch shows the boundary between the metamorphic Southalpine Basement and the assumed "non-metamorphic" sequence of the Carnic Chain taken from the literature (METAMORPHIC MAP OF THE ALPS, 1973; STRUCTURAL MODEL OF ITALY AND GRAVITY MAP, 1990) (VB = Val Bordaglia Line, PL = Pusteria Line, TC = Tröpolach-Camporosso Line). Sample location: 1 = *CHS*, 2 = *CHN*, 3 = *FR*, 4 = *SI*, 5 = *RI*, 6 = *CO*, 7 = *SD*, 8 = *PA*, 9 = *PS* (see Tab. 1).

through Bressanone-Pusteria to Comelico; (ii) an intermediate, approximately southwest–northeast trending belt, from Valsugana through Cima d'Asta to Agordo; (iii) a southern area, the Recoaro-Schio area. The MSB only records Variscan metamorphism. The main structures are Variscan in age, but Alpine structures also occur (mostly gentle folding and brittle deformation). The mineral assemblages occurring in MSB display greenschist facies conditions, with a metamorphic zoning including an almandine zone (mainly localized in the north-western part of MSB), a biotite zone, and, in the southernmost and easternmost part, a chlorite zone.

The MSB passes eastwards to the anchizonal or even non-metamorphic Paleozoic sequences of the Carnic Alps, in which a Variscan Paleocarnic Chain has been recognized (SPALLETTA et al., 1982; VAI et al., 1984; VENTURINI, 1990). The relationships between the MSB and the Paleozoic sequences of the Carnic Alps are rather complex from the structural point of view, due to the overlapping effects of complicated Variscan plus Alpine tectonics.

The Paleocarnic Chain (PCC for short) consists of a narrow, west-east elongated belt outcropping in Comelico and in Carnia. Its deformational history records strong multistage Variscan compressions. Furthermore, the Alpine orogeny also produced an intense, mainly north–south shortening. During the last decade the Variscan deformations have been successfully distinguished from the Alpine ones in several Lower Paleozoic sedimentary nuclei (VENTURINI, 1990, 1991; VENTURINI and DELZOTTO, 1992).

Metamorphic effects, where present in the PCC, are reported to have a very low grade and to be of Variscan age. The Alpine tectonic reworking of the PCC was not accompanied by metamorphism. However, as pointed out in the introduction, considering the pre-Upper Carboniferous complexes of the Southern Alps (i.e. MSB + PCC) as a whole, the location of the boundary between the metamorphic and non-metamorphic domains is still unknown. Contrasting results are reported in the literature about this question: (i) large scale maps localize this boundary as shown in figure 1; (ii) new analytical data (ÁRKAI et al., 1991) indicate that this location is wrong; the boundary should occur to the east of the western slope of Hocheck (i.e. to the east of the meridian of Kartisch).

The PCC can be subdivided into two main adjacent areas, each characterized by a different lithology: (i) the western sector coincides with the Comelico metamorphic sequences, which strictly belong to the MSB representing its easternmost part; (ii) the eastern sector includes several fossiliferous sequences, ranging from Upper Ordovician to Visean. Both sectors are capped by a non-metamorphic Permo-Carboniferous and/or Permo-Scythian sedimentary cover, through a well exposed angular unconformity. The ranges of sedimentation age within these two sectors are given in SASSI et al. (1994, and references quoted therein) for MSB and in SPALLETTA et al. (1982), VENTURINI, 1990, and LÄUFER et al. (1993) for PCC. It must be emphasized that, at a regional scale, a metamorphic hiatus between the pre-Upper Carboniferous sequences and the post-Variscan cover has been reported (MENEGAZZI et al., 1991).

The Val Bordaglia Line (Fig. 1) is the major tectonic element in the considered area of the Southern Alps. It consists of a N50°E trending bundle of subvertical faults which first became active during Late Carboniferous and then were re-activated during the Alpine compressive phases (VENTURINI and DELZOTTO, 1992).

Several other tectonic lines and thrust planes occur in the area, so that the rock sequences in the easternmost part of the MSB and the PCC within the area of figure 1 are dismembered in several tectonic units, due to combined effects of Variscan and Alpine tectonics. Therefore, the thermal zone (i.e. epizone, anchizone, diagenetic zone) assigned to a given rock sequence in a specific locality cannot be extrapolated in an offhand manner, but only after having taken into due consideration the many constraints imposed by the complicated structure of this area. For this reason, some details on the structure of the area to the east of the Val Bordaglia Line are necessary to be explained.

In Carnia the Variscan orogeny produced a complex structural pattern trending, at present, N120°E. The folded and thrust edifice can be considered a foreland fold-thrust belt uplifted in a short time span (not before Namurian and not after Westfalian B). This deformation phase is the Carnic event (VAI, 1976; VENTURINI, 1991). It reflects the Leonian movements connected to the Asturian phase. Field evidence confirms that the Carnic area only underwent this youngest Variscan deformational phase. It produced three different deformation styles (VENTURINI, 1990, 1991) which overprinted each other and are characterized by the same N120°E trend with south-southwestern vergence. Each system of structures is to be referred to a shallower crustal depth of burial supported by the accreting belt during its deformation history (Fig. 2).

The first and deepest deformation stage developed a multi-km asymmetric close fold almost

as wide as the entire north–south section of the presently outcropping belt (Fig. 2A).

The second and shallower deformation stage produced many ramp and flat structures which intersected and shifted the previous macro-fold producing a thick system of tectonic slices (Fig. 2 B, C). It corresponds to the "imbricated tectonic slices" recognized by SELLI (1963), VAI (1979) and SPALLETTA et al. (1982) as the only Variscan structures of the PCC.

The third and shallowest deformation stage took place after a further uplift of the PCC. A series of km-size, open antiforms developed along newly-formed mega-thrust surfaces. All the previous structures were refolded (Fig. 2D).

Paleomagnetic data from the overlying Permo-Carboniferous beds, which unconformably rest on the Variscan folded belt, indicate that the Variscan substratum has been rotated counterclockwise by about 40° since Upper Carboniferous (MANZONI et al., 1989). This rotation is quite similar to that measured in the Comelico and in the Dolomites (MANZONI, 1970). Therefore, both the Carnia and Comelico structural trends rotated together since the end of the Variscan orogeny.

As pointed out above, the Val Bordaglia Line (N50°E trending) is the major tectonic line in this area. The ancestral significance of this line is very important for better understanding the geological meaning of the petrographic results of the present paper. Two different hypotheses have been proposed for the first activation of the Val Bordaglia Line: (i) ZANFERRARI and POLI (pers. comm.) interpret the Variscan deformations of the Carnic area as induced by the overthrust of the Comelico metamorphic units along a Variscan N30°–50°E trending thrust, the northern portion of which is supposed to correspond to the Val Bordaglia Line; this hypothesis seems to conflict with the N120°E structures occurring both in Carnia and Comelico; (ii) in contrast, VENTURINI (in CASSINIS et al., 1993) proposes that the first activation of the Val Bordaglia Line was due to the strike slip transcurrent movements which induced, along this line, a contractional duplex developed in restraining overstep conditions. These movements should have occurred at the very end of the Variscan phase, during the Late Variscan wrench tectonics. Their effects were the exhumation of the western low-grade metamorphic units

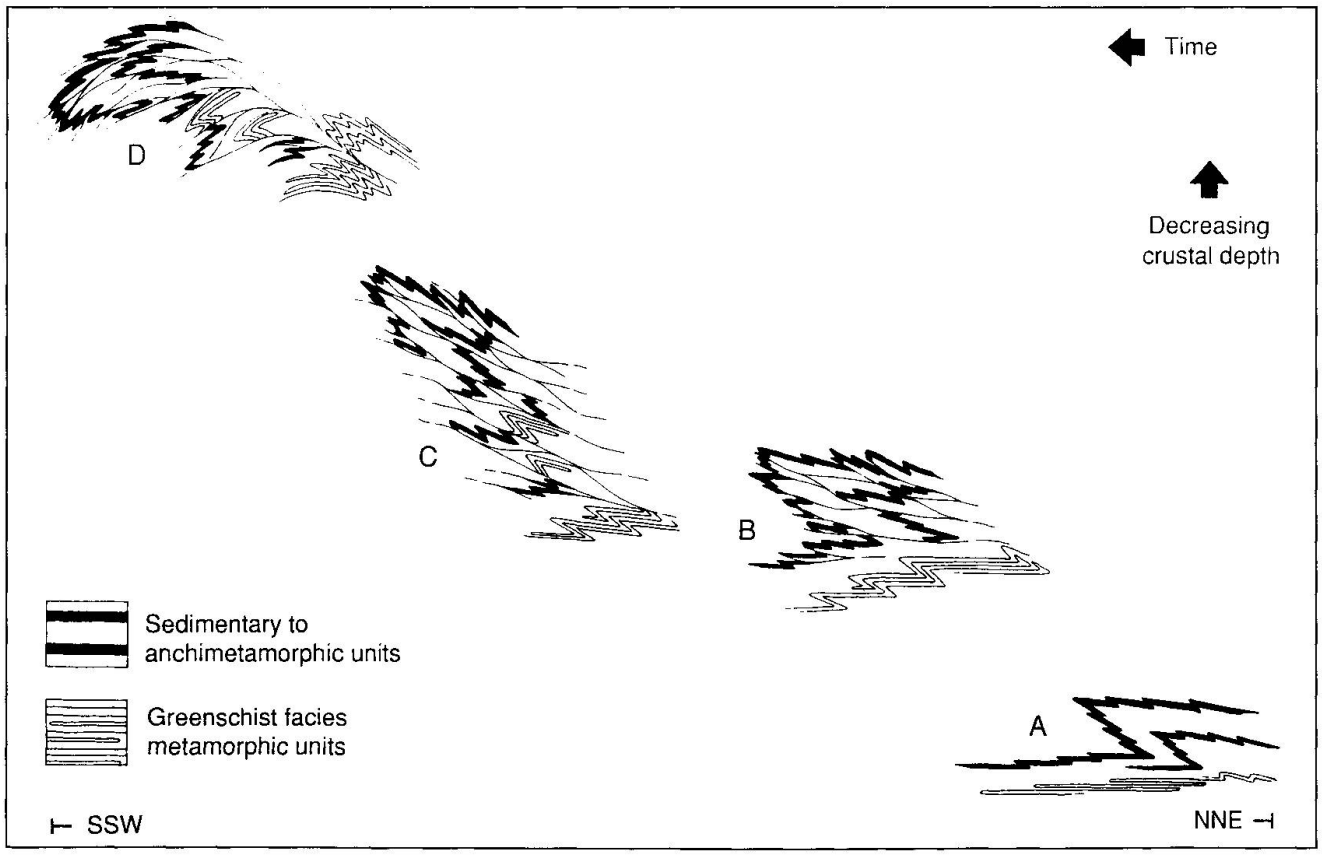


*Fig. 2* Effects of the three deformation stages of the Carnic event (A to D) in the Carnic Alps, east of the Val Bordaglia Line (see text). This interpretation tries to explain the mixture between sedimentary and metamorphic (epizonal) units (from VENTURINI, 1991, modif.). A = 1st stage; B, C = 2nd stage; D = 3rd stage.

*Tab. 1* Sites of the nine sample groups and their stratigraphic classification.

| Sample group | Sites (see Fig.1) | Formation | Locality |
|---|---|---|---|
| *CHS* | 1 | Val Visdende | M.te Chiadenis (Sud) |
| *CHN* | 2 | ValVisdende | M.te Chiadenis (Nord) |
| *FR* | 3 | Hochwipfel | Frassenetto |
| *SI* | 4 | Hochwipfel | Sigilletto |
| *RI* | 5 | Hochwipfel | Rigolato-Forni Avoltri |
| *CO* | 6 | Dimon | Comeglians |
| *SD* | 7 | Dimon | Moscardo (Paluzza) |
| *PA* | 8 | Hochwipfel | Paularo |
| *PS* | 9 | Dimon | Paularo (Sud) |

(Comelico) and their contemporaneous translation over mainly non-metamorphic sequences (Carnia).

## The rock samples

Nine sites were selected following structural criteria, and ca. 30 rock samples were collected in each site from a single big outcrop. Therefore, a sample population of 256 rock samples of pelitic to silty composition was obtained, consisting of nine sample groups each related to a given site as specified in figure 1 and table 1. They represent three formations:

– The Val Visdende Formation which consists of metapelites and minor interlayered metapsammites. Its age is still controversial: some authors consider it as Lower Ordovician, but others, based on the assumption of a lithological equivalence with the Hochwipfel Formation, as Lower Carboniferous.

– The Hochwipfel and Dimon formations make up the so-called Hercynian Flysch and represent the youngest units of the Hercynian sequence of the Paleocarnic Chain.

After a standard petrographic analysis of some thin sections from each outcrop, all samples have been used for an estimate of the thermal zone (in terms of epizone, anchizone, diagenetic zone) by means of measurements of the illite "crystallinity" and vitrinite reflectance, and an estimate of the pressure character of metamorphism by means of measurements of the $d_{33\bar{1},060}$ spacing of potassic white mica.

## Analytical procedures

*(i) Illite "crystallinity":* Illite "crystallinity" (IC) was determined by X-ray diffractometry (XRD), using the procedures and criteria proposed by KÜBLER (1968, 1975, 1990).

The rock samples were disaggregated under standard conditions using a jaw crusher followed by crushing in a mortar mill (type Pulverisette 2, Fritsch) for three minutes. Previous experiments showed that this short-term pulverization has no measurable effects on the IC values. Final disaggregation was achieved by repeated shaking in deionized water. The < 2 μm grain-size fraction was separated from aqueous suspension based on differential settling of grains of different diameters. Aqueous suspensions of the given fraction were pipetted and dried at room temperature on glass slides to produce thin-layer, highly orientated preparations. Results from the literature on the possible effects of material amounts (thickness) of the sedimented preparations on IC values are rather controversial (see the review of LEZZERINI et al., 1995). As to our former results (ÁRKAI, 1982), statistically comparable IC values can be obtained using mounts with material loads between 1 and 3 mg/cm$^2$.

A Philips PW-1730 diffractometer was used at 45 kV / 35 mA, with $CuK_\alpha$ radiation, graphite monochromator, proportional counter, divergence and detector slits of 1°, goniometer speed of $^1/_2$°/min, time constant of 2 s, and chart speed of 2 cm/min. At these instrumental parameters, the standard deviation of the half-height width measurements was $s = 0.008\ \Delta°2\Theta$ (n = 10) for an IC of 0.215 °2Θ.

The calibration of IC values against those of Kübler's laboratory (where the 0.25–0.42 Δ°2Θ boundary values of the anchizone were established) was made using standard rock slabs (series Nos 32, 34 and 35) kindly provided by B. Kübler. Smaller scale, temporary instrumental changes were corrected by the repeated use of a calibrated standard rock slab series (Nos Á-1, –2 and –3) of the Laboratory for Geochemical Research, Budapest. Applying the least-square method, the calibration equations is:

$$IC(\text{Kübler}) = 1.164 \times IC(_{\text{present work}}) - 0.038.$$

Thus, IC values of 0.247 and 0.393 Δ°2Θ correspond to the Kübler's anchizone boundaries in the present paper.

*(ii) Vitrinite reflectance:* Vitrinite reflectance ($R_{max}$, $R_{min}$) of the dispersed, coalified particles were measured in the Institute of Coal and Petroleum of the Technical University Aachen, Germany by means of a Zeiss microscope with EPI

*Tab. 2* Statistical parameters of the illite "crystallinity" (IC) data and illite-muscovite basal spacing values calculated from the (00,10) peak ($x$ = average; $s$ = standard deviation; $s(x)$ = standard error ($s/\sqrt{n}$; $s\%$ = standard deviation expressed in percentage of the average; $n$ = number of data). The groups are listed in order of increasing IC mean value.

| Sample | IC | | | | | d(002) | | | | |
|---|---|---|---|---|---|---|---|---|---|---|
| group | $x$ | $s$ | $s\%$ | $s(x)$ | $n$ | $x$ | $s$ | $s\%$ | $s(x)$ | $n$ |
| *CHN* | 0.184 | 0.015 | 8.17 | 0.003 | 28 | 9.966 | 0.012 | 0.118 | 0.002 | 28 |
| *CHS* | 0.195 | 0.017 | 8.67 | 0.003 | 30 | 9.966 | 0.010 | 0.095 | 0.002 | 30 |
| *RI* | 0.222 | 0.014 | 6.42 | 0.003 | 30 | 9.951 | 0.007 | 0.074 | 0.001 | 29 |
| *SD* | 0.242 | 0.029 | 12.05 | 0.007 | 18 | 9.978 | 0.009 | 0.087 | 0.002 | 18 |
| *PS* | 0.256 | 0.017 | 6.56 | 0.003 | 32 | 9.947 | 0.007 | 0.069 | 0.001 | 32 |
| *SI* | 0.265 | 0.020 | 7.46 | 0.004 | 29 | 9.960 | 0.008 | 0.081 | 0.002 | 27 |
| *CO* | 0.293 | 0.026 | 8.89 | 0.005 | 30 | 9.978 | 0.009 | 0.088 | 0.002 | 30 |
| *PA* | 0.303 | 0.025 | 8.13 | 0.005 | 30 | 9.971 | 0.013 | 0.129 | 0.002 | 30 |
| *FR* | 0.380 | 0.040 | 10.58 | 0.007 | 29 | 9.996 | 0.014 | 0.136 | 0.003 | 28 |

40× objective in oil immersion [n(23 °C, e) = 1.518], using as standard an Y-Al-garnet having a reflectance of R = 0.88%. The results were checked by repeated measurements on some rock samples, using the reflectance glass prism series of the Bituminous Coal Research Inc. as reference standards. Convincingly good fit was found between the data-set pairs.

*(iii) Measurement of the $d_{33\bar{1},060}$ spacing:* Following the analytical procedure proposed by SASSI (1972) and SASSI and SCOLARI (1974), the values of $d_{33\bar{1},060}$ spacing of K white mica were measured for monitoring pressure in samples having a suitable bulk and mineral composition, according to the criteria also explained by GUIDOTTI and SASSI (1976, 1986) and RIEDER et al. (1992). According to SASSI and SCOLARI (1974), this spacing is measured directly from rock slices cut perpendicularly to the rock foliation. Metallic silicon, added to the rock slices by filling in thin drilled grooves, and quartz of the rock were used as standards. The analytical error is ± 0.002 Å.

*Tab. 3* Significance test of the difference between IC averages ($x$ = average difference betweeen the averages; bold character: significant difference at P = 1%; normal character: insignificant difference at P = 1%; values in parentheses: minimum significant differences between the given groups at P = 1%).

| groups | *CHS* | *CHN* | *FR* | *SI* | *RI* | *CO* | *SD* | *PS* | *PA* |
|---|---|---|---|---|---|---|---|---|---|
| $x$ | 0.195 | 0.184 | 0.380 | 0.265 | 0.222 | 0.293 | 0.242 | 0.256 | 0.303 |
| *PA* | **0.108** *(0.015)* | **0.119** *(0.015)* | **0.077** *(0.024)* | **0.038** *(0.016)* | **0.081** *(0.014)* | 0.010 *(0.017)* | **0.061** *(0.021)* | **0.047** *(0.014)* | |
| *PS* | **0.061** *(0.011)* | **0.072** *(0.011)* | **0.124** *(0.022)* | 0.009 *(0.012)* | **0.034** *(0.011)* | **0.037** *(0.015)* | 0.014 *(0.022)* | | |
| *SD* | **0.047** *(0.022)* | **0.058** *(0.021)* | **0.144** *(0.023)* | **0.023** *(0.019)* | 0.020 *(0.021)* | **0.051** *(0.022)* | | | |
| *CO* | **0.098** *(0.015)* | **0.109** *(0.015)* | **0.087** *(0.023)* | **0.028** *(0.016)* | **0.071** *(0.015)* | | | | |
| *RI* | **0.027** *(0.011)* | **0.038** *(0.010)* | **0.158** *0.022)* | **0.043** *(0.012)* | | | | | |
| *SI* | **0.070** *(0.013)* | **0.081** *(0.012)* | **0.115** *(0.023)* | | | | | | |
| *FR* | **0.185** *(0.022)* | **0.196** *(0.022)* | | | | | | | |
| *CHN* | 0.011 *(0.011)* | | | | | | | | |

*Tab. 4* Significance test of differences between d(002) averages of illite-muscovite calculated from the d(00,10) values (symbols as in Tab. 2).

| groups | *CHS* | *CHN* | *FR* | *SI* | *RI* | *CO* | *SD* | *PS* | *PA* |
|---|---|---|---|---|---|---|---|---|---|
| *x* | 9.966 | 9.966 | 9.995 | 9.960 | 9.951 | 9.978 | 9.977 | 9.946 | 9.971 |
| *PA* | 0.005 *(0.008)* | 0.005 *(0.008)* | **0.024** *(0.009)* | **0.011** *(0.008)* | **0.020** *(0.008)* | 0.007 *(0.008)* | 0.006 *(0.009)* | **0.025** *(0.007)* | |
| *PS* | **0.020** *(0.005)* | **0.020** *(0.007)* | **0.049** *(0.008)* | **0.014** *(0.005)* | 0.005 *(0.005)* | **0.032** *(0.005)* | **0.031** *(0.006)* | | |
| *SD* | **0.011** *(0.007)* | **0.011** *(0.009)* | **0.018** *(0.010)* | **0.017** *(0.007)* | **0.026** *(0.006)* | 0.001 *(0.007)* | | | |
| *CO* | **0.012** *(0.006)* | **0.012** *(0.007)* | **0.017** *(0.008)* | **0.018** *(0.006)* | **0.027** *(0.006)* | | | | |
| *RI* | **0.015** *(0.006)* | **0.015** *(0.007)* | **0.044** *(0.008)* | **0.009** *(0.005)* | | | | | |
| *SI* | **0.006** *(0.006)* | 0.006 *(0.007)* | **0.035** *(0.003)* | | | | | | |
| *FR* | **0.029** *(0.008)* | **0.029** *(0.009)* | | | | | | | |
| *CHN* | 0.000 *(0.007)* | | | | | | | | |

## Analytical results

The results obtained using the above methods and procedures are described and discussed below, in terms of: (i) modal composition of the fraction having a grain size < 2 μm; (ii) IC results and their regional variation; (iii) coal rank results and their regional variation; (iv) barometric estimate based on the value of $d_{33\bar{1},060}$.

### MODAL COMPOSITION OF THE < 2 μm GRAIN-SIZE FRACTION

Based on the XRD analyses, white mica (illite-muscovite) and chlorite predominate in the < 2 μm grain size fraction samples, while the amounts of quartz, albite and rutile are subordinate in most of the sample groups. Na-bearing white micas, forming mostly paragonite/muscovite mixed-layer and rarely discrete paragonite flakes, were detected as traces in the sample groups *CHS, CHN, FR, RI, SD, PS* and *PA*, being most frequent in the groups *FR* and *PS*, rare in the groups *CHN, SD*, and sporadic in the groups *CHS, RI* and *PA*. In the sample group *FR* a negative correlation was found between the amount of albite and that of the paragonitic phases.

The sample group *SD* is the only one in which quartz is more abundant than chlorite.

Other phyllosilicates, such as kaolinite in one sample of group *CHS*, smectite in one sample of group *FR*, and mixed-layer illite/smectite in four samples of group *SI*, as well as goethite in group *SD* are non-metamorphic phases, but are related to a slight, post-metamorphic, weathering.

The metamorphic mineral phases occurring in the < 2 μm fraction are illite-muscovite, chlorite, quartz ± albite, mixed-layer paragonite/muscovite, paragonite and rutile. This mineral assemblage is stable from the deep diagenetic zone through the whole anchizone up to the chlorite zone of the greenschist facies. Therefore, a precise determination of the metamorphic grade can only be obtained from illite "crystallinity" (IC) data.

### REGIONAL VARIATIONS OF IC RESULTS

The statistics of the IC values are shown in table 2. Before discussing the differences in metamorphic grade between the different sample groups, the possible effects of the paragonite content on the IC values should be evaluated, because the occurrence of paragonite as a discrete phase and/or as mixed-layers with illite-muscovite may broaden significantly the 10 Å reflection of the latter phyllosilicate. As mentioned above, paragonite and paragonite/muscovite occur only as traces in the analyzed samples. For their identifica-

tion and discrimination from margarite in the presence of predominating illite-muscovite, the (00,10) reflections near 2 Å were used, following FREY and NIGGLI (1972). Although the largest IC average was obtained from the sample group *FR* in which the paragonitic phases are most frequent, no significant relationship was found between the abundance of paragonitic phases and the IC values, because some groups (e.g. *CHN, CHS, SD*) with very small IC averages contain paragonitic phases, while others (*SI, CO*) in which Na-mica is lacking, are characterized by larger IC averages. Consequently, possible effects of paragonitic phases on the IC values can be ignored. Furthermore, rock bulk composition is identical both within each group and among the different sample groups: this feature was indeed a pre-requisite in sample collection and sample selection, and was tested both in thin sections and by means of X-ray powder diffractometry. Finally, the frequency distribution of the IC data in each analyzed sample group is near to normal. Therefore, the IC averages only monitor the metamorphic grade, and thus can be used for establishing the thermal zones as well as differences in metamorphic grade.

Epizonal IC average values were obtained from the groups *CHS, CHN, RI* and *SD*. Among them, lowest IC value (i.e. the highest metamorphic grade) was found in *CHN*, the highest IC value (i.e. the lowest metamorphic grade) in group *SD*, indicating a moderate decrease of metamorphic temperature eastwards within these epizonal sample groups.

High-T anchizonal (near to the anchi-/epizone boundary) conditions were deduced from the IC average values of groups *PS* and *SI*, while medium-T anchizonal conditions are recorded in the groups *CO* and *PA*. The IC average of group *FR* corresponds to the lowest T part of the anchizone, being very close to the IC boundary between the diagenetic zone and the anchizone. Thus, it represents the lowest temperature recorded in the investigated sample groups. Therefore, the commonly assumed non-metamorphic Paleozoic sequences of PCC are anchimetamorphic indeed.

The above mentioned analytical results and their interpretation do not display a regular transitional trend but, as expected, a variation of the temperature conditions which can be understood only if the complex regional structure is taken into

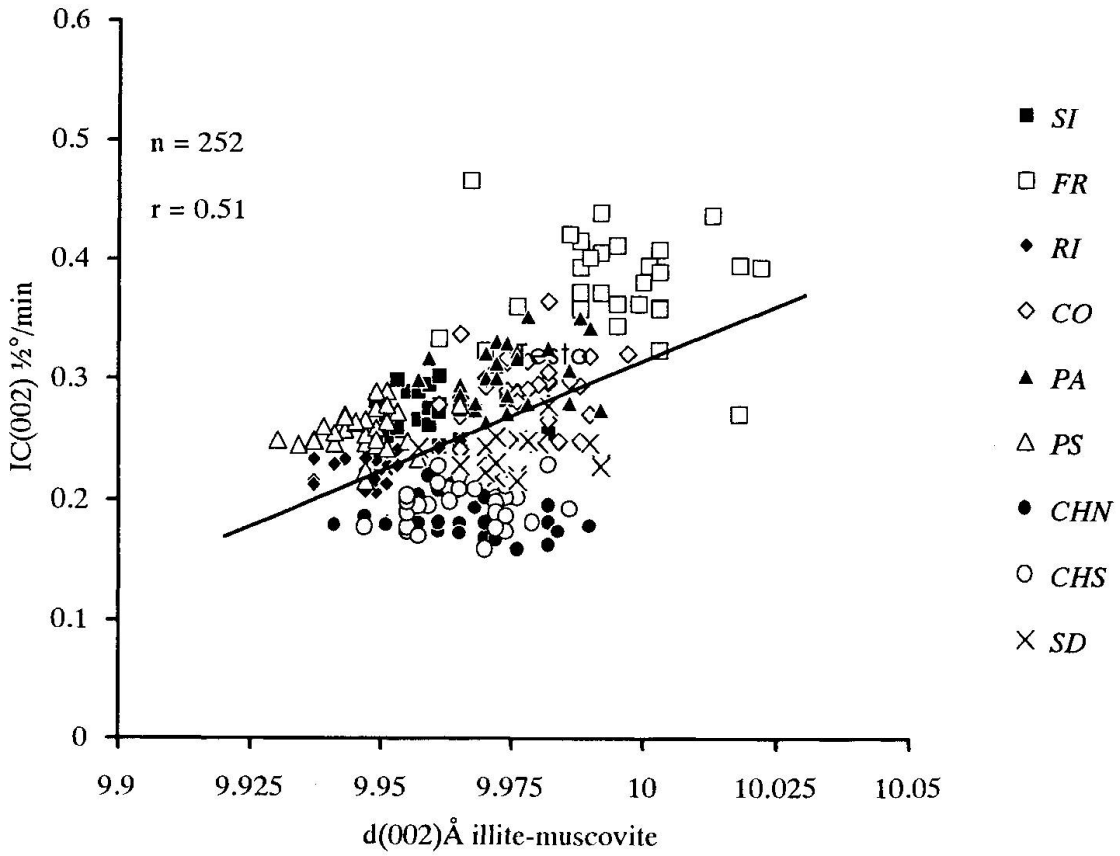


*Fig 3* Moderate, but significant (at P = 1%; r = 0.51) positive correlation between d(002) and IC data, both based on measurements at $^1/_2$°/min goniometer speed.

*Tab. 5* Average maximum and minimum reflectance ($R_{max}$, $R_{min}$) and bireflectance ($\Delta R = R_{max} - R_{min}$) of the huminite-type dispersed organic matter ($n$ = number of measurements, $s$ = standard deviation, $s(x)$ = standard error).

| Sample group | No. | $n$ | $R_{max}$(%) | $s$ | $s(x)$ | $R_{min}$(%) | $s$ | $s(x)$ | $\Delta R$(%) |
|---|---|---|---|---|---|---|---|---|---|
| *CHN* | 290 | 5 | 9.38 | 0.78 | 0.35 | 0.82 | 0.15 | 0.07 | 8.56 |
| | 305 | 12 | 7.53 | 0.67 | 0.20 | 1.34 | 0.43 | 0.13 | 6.19 |
| *CHS* | 327 | 10 | 7.15 | 1.32 | 0.42 | 0.81 | 0.30 | 0.10 | 6.34 |
| *SI* | 101 | 20 | 5.62 | 0.42 | 0.10 | 4.02 | 0.58 | 0.13 | 1.59 |
| | 103 | 30 | 5.45 | 0.45 | 0.08 | 3.31 | 0.51 | 0.09 | 2.14 |
| | 108 | 20 | 5.54 | 0.60 | 0.13 | 3.97 | 0.84 | 0.19 | 1.57 |
| | 113 | 40 | 5.32 | 0.22 | 0.03 | 3.94 | 0.44 | 0.07 | 1.39 |
| | 121 | 20 | 3.76 | 0.29 | 0.07 | 2.52 | 0.40 | 0.09 | 1.24 |
| | 123 | 20 | 6.07 | 0.50 | 0.11 | 3.43 | 0.66 | 0.15 | 2.64 |
| | 124 | 25 | 5.97 | 0.77 | 0.15 | 3.63 | 0.74 | 0.15 | 2.35 |
| *CO* | 191 | 30 | 5.27 | 0.34 | 0.06 | 3.69 | 0.47 | 0.09 | 1.58 |
| | 193 | 13 | 5.17 | 0.30 | 0.08 | 4.24 | 0.63 | 0.18 | 0.93 |
| | 196 | 20 | 5.20 | 0.29 | 0.06 | 4.31 | 0.61 | 0.14 | 0.89 |
| | 198 | 5 | 9.18 | 0.55 | 0.25 | 0.86 | 0.16 | 0.07 | 8.32 |
| | 205 | 15 | 4.92 | 0.41 | 0.11 | 3.49 | 0.35 | 0.09 | 1.43 |
| | 212 | 20 | 4.92 | 0.20 | 0.05 | 4.27 | 0.29 | 0.07 | 0.65 |
| | 217 | 20 | 5.08 | 0.21 | 0.05 | 4.15 | 0.37 | 0.08 | 0.93 |
| *PA* | 221 | 14 | 3.96 | 0.57 | 0.15 | 2.62 | 0.63 | 0.17 | 1.35 |
| | 227 | 18 | 3.93 | 0.24 | 0.06 | 2.72 | 0.53 | 0.13 | 1.21 |
| | 232 | 20 | 3.79 | 0.36 | 0.08 | 2.67 | 0.47 | 0.10 | 1.12 |
| | 240 | 20 | 3.89 | 0.28 | 0.06 | 2.90 | 0.40 | 0.09 | 0.99 |
| | 243 | 20 | 3.88 | 0.26 | 0.06 | 2.79 | 0.55 | 0.12 | 1.08 |
| *FR* | 131 | 3 | 7.93 | 0.21 | 0.12 | 1.44 | 0.31 | 0.18 | 6.49 |
| | 136 | 6 | 8.70 | 1.06 | 0.43 | 0.92 | 0.11 | 0.04 | 7.79 |
| | 144 | 4 | 6.16 | 0.27 | 0.13 | 0.69 | 0.15 | 0.07 | 5.46 |
| | 144a | 7 | 5.76 | 0.81 | 0.31 | 2.17 | 0.60 | 0.23 | 3.59 |
| | 151 | 11 | 7.06 | 0.59 | 0.18 | 1.06 | 0.36 | 0.11 | 5.00 |
| | 156 | 19 | 6.13 | 0.86 | 0.20 | 1.32 | 0.71 | 0.16 | 4.82 |
| | 157 | 5 | 9.09 | 0.87 | 0.39 | 0.89 | 0.19 | 0.08 | 8.20 |

consideration, as emphasized in the concluding remarks. In any case, in order to decide whether the differences observed between the IC average values of the sample groups may or may not have a real geologic meaning, statistical significance tests of these differences were carried out for all possible group-pairs. For this aim, the mean ($x$), the confidence limits of the mean ($x_{min}$, $x_{max}$) at $P$ = 1% significance level (i.e., at 99% probability), the standard deviation ($s$) and the standard error [$s(x) = s/\sqrt{n}$] were calculated for each group. When comparing the averages of two groups by $t$-test, different algorithms were used for cases $n_1 \gtrless n_2$. The algorithms were also modified depending on the results of the $f$-test carried out previously to check whether the standard deviations of the compared groups were significantly different or not (at the same significance level). The home-compiled program used for these purposes calculates the difference of the averages, indicates whether this difference is significant or not at a given level (in our case at P = 1%), and also gives the value of the minimum significant difference at the same P, the standard deviation and the confidence limits of the difference.

Table 3 displays the main results of this statistical analysis. Most of the IC differences found between the various sample group pairs turn out to be significant at P = 1% level. When the differences in a group pair are not significant, it means that the considered sample groups record similar metamorphic conditions. This is the case of the epizonal *CHS-CHN* and *RI-SD* pairs, as well as of the anchizonal *CO-PA* and *SI-CO* pairs. It is worthy to point out the strong similarity between the groups *SD* and *PS*, although the former one belongs to the epizone, the latter one to the high-T part of the anchizone. This fact is due to the arbitrary nature of the zone boundaries based on IC values.

The values of the basal spacing in the < 2 μm fraction has been also measured. Table 2 shows

the results obtained from the d(00,10) reflection and their statistics. The d(002) values range between 9.947 and 9.996 Å. Based on the results of the significance tests of the differences (Tab. 4), the d(002) averages of the group pairs *CHS-CHN, CHS-PA, CHN-SI, CHN-PA, RI-PS, CO-SD, CO-PA* and *SD-PA* turn out to be similar, while all others are different at P = 1%. No correlation was found between the d(002) average values and the occurrences of paragonite and/or mixed-layer paragonite/muscovite. Both the lowest and the highest d(002) average values were found in groups *PS* and *FR*, in which paragonitic phases most frequently occur. A moderate, but significant positive correlation (r = 0.51; the confidence limits of 0.51 are 0.56 and 0.30 at P = 1%) was found between the d(002) and IC averages (Fig. 3). With decreasing IC (i.e., with increasing metamorphic grade) the d(002) of illite-muscovite also decreases, which may be a consequence of increasing Na content in the K-white mica structure (GUIDOTTI and SASSI, 1976; GUIDOTTI et al., 1992).

*Tab. 6* Statistical parameters of the $6d_{33\bar{1},060}$ dimension (*m* = prevailing mica population, newly formed during the main phase of the Variscan metamorphism; *d* = subordinate mica population of possible detrital or/and Alpine overprinting origin; other symbols as in table 2).

| Sample Group | | n | x (Å) | s |
|---|---|---|---|---|
| *CHN* | *m* | 25 | 8.997 | 0.010 |
| | *d* | 10 | 9.008 | 0.004 |
| *CHS* | *m* | 28 | 9.003 | 0.006 |
| *RI* | *m* | 13 | 8.990 | 0.006 |
| | *d* | 30 | 9.022 | 0.004 |
| *SD* | *m* | 17 | 8.992 | 0.007 |
| *PS* | *m* | 10 | 8.988 | 0.005 |
| | *d* | 30 | 9.022 | 0.003 |
| *SI* | *m* | 23 | 8.993 | 0.010 |
| | *d* | 15 | 9.016 | 0.004 |
| *CO* | *m* | 25 | 8.986 | 0.005 |
| *PA* | *m* | 22 | 8.996 | 0.009 |
| | *d* | 15 | 9.019 | 0.006 |
| *FR* | *m* | 25 | 8.983 | 0.003 |
| *tot* | *m* | 188 | 8.992 | 0.009 |
| | *d* | 90 | 9.019 | 0.006 |

## REGIONAL VARIATION OF COAL RANK RESULTS

Dispersed, coalified organic matter with measurable grain size was found only in samples that belong to groups *CHN, CHS, SI, CO* and *FR*. Its maximum and minimum reflectance and bireflectance values are shown in table 5.

High $R_{max}$ (> 7.1%), low $R_{min}$ (< 1.4%) and high $\Delta R$ (> 6.1%) values were found in the groups *CHN* and *CHS*, displaying epizonal character consistently with the IC data.

In contrast, significantly lower $R_{max}$, higher $R_{min}$ and lower $\Delta R$ values were obtained in the groups *SI, CO* and *PA*, revealing a lower grade, i.e. an anchizonal character, again in a fairly good agreement with the IC data. For the high-T anchizonal group *SI* (as classified on the basis of IC data) the $R_{max}$ and $\Delta R$ values are higher (3.8–6.1% and 1.2–2.6%, respectively) than those of the groups *CO* and *PA*, which are medium-T anchizonal on the basis of the IC data.

Anomalously high $R_{max}$, low $R_{min}$ and high $\Delta R$ values were obtained for the group *FR*, which is the lowest grade group (low-T anchizone, near to the anchizone/diagenetic zone boundary) based on IC data ($R_{max}$ = 5.8–9.1%, $R_{min}$ = 0.7–1.4%, $\Delta R$ = 3.6–8.2%). This discrepancy may be interpreted differently:

(i) the overwhelming part of the organic matter grains in *FR* could be derived as thermally matured detritus from higher-grade metamorphic rocks;

(ii) it may have suffered a short-term magmatic heating, which did not affect IC;

(iii) it may have suffered a short-term tectonic heating and deformation, which did not affect IC.

Hypothesis (ii) is not realistic from the geological point of view, and the style of rock deformation in the locality *FR*, does not differ significantly from that of the other localities. Therefore the hypothesis (i) seems to be the most probable at present.

## BAROMETRIC ESTIMATE BASED ON THE $d_{33\bar{1},060}$ VALUE OF POTASSIC WHITE MICA

233 samples of metapelites of appropriate composition from the nine localities were taken into consideration for geobarometric purposes. The geobarometric method based on the $d_{33\bar{1},060}$ spacing of potassic white micas was originally proposed and calibrated in the lower part of the greenschist facies (SASSI, 1972; SASSI and SCOLARI, 1974; GUIDOTTI and SASSI, 1976, 1986), but was then extended to very low-grade rocks by PADAN et al. (1982).

FREY (1987) and ESSENE (1989) suggested some caution on the use of this method; however,

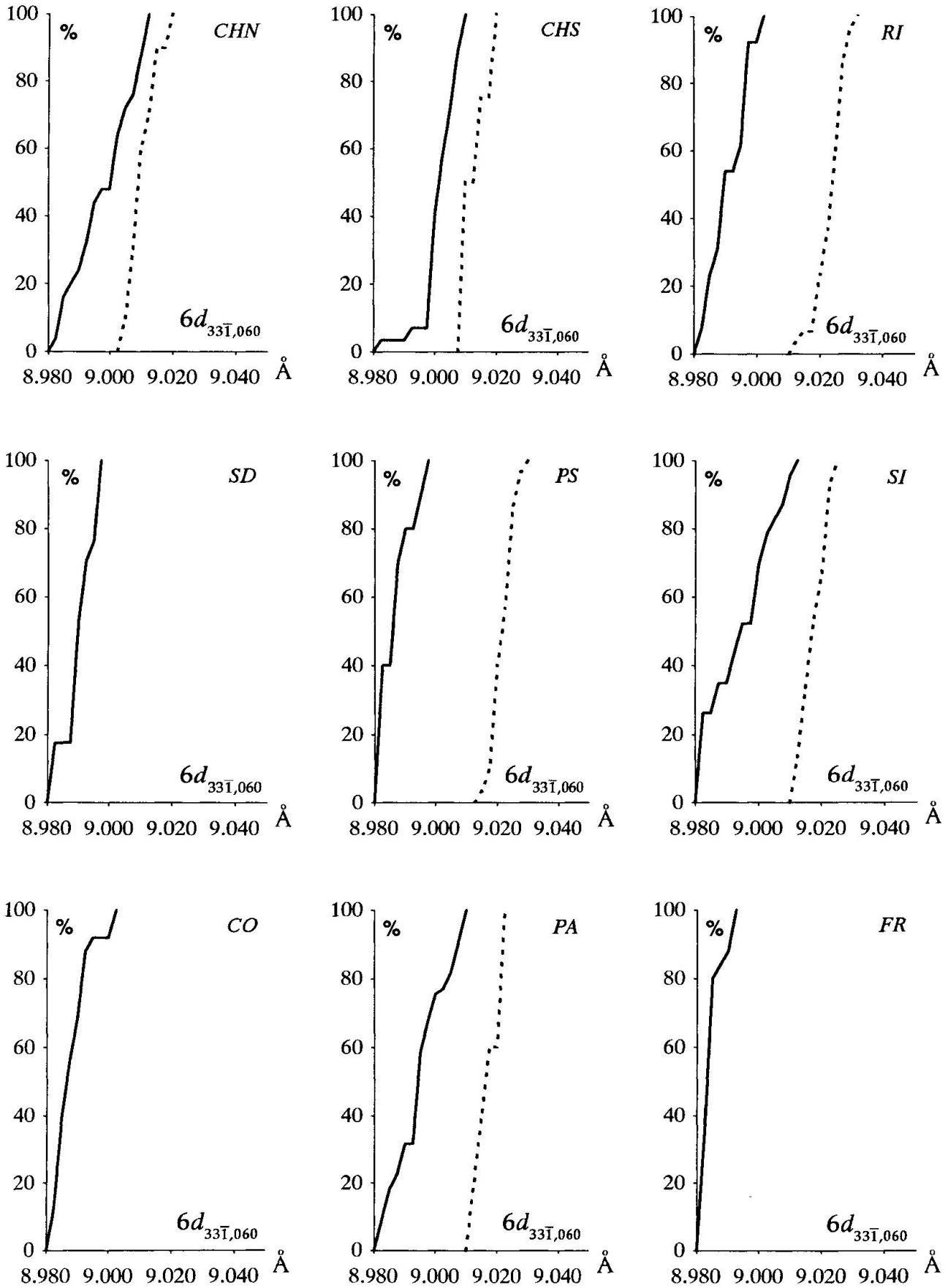


*Fig. 4* Cumulative frequency curves of the $6d_{33\bar{1},060}$ value for each group: the solid line corresponds to the newly formed Variscan micas, the dashed one to assumedly detrital or Alpine overprinting micas.

the analytical procedure and the solid petrologic frame developed by GUIDOTTI and SASSI (1976, 1986) prevent the claimed risks.

278 measurements were carried out. As shown in table 6 and in figure 4, most sample groups indicate the existence of two mica populations, one quantitatively prevailing over the other, as deduced from the intensities of the $d_{33\bar{1},060}$ peak. The splitting of this peak is certainly not related to the $\alpha_1$–$\alpha_2$ doublet, because the distance between the two peaks is not constant, as clearly shown in figure 4.

The prevailing mica is to be considered as newly formed in these rocks (i.e. metamorphic), consistent with microstructural observation and XRD measurements on several, < 2 μm grain-size fraction samples. The other micas, which occur in low amounts and may also be lacking, are rather problematic, because their interpretation is ambiguous. They could represent detrital mica flakes, the occurrence of which has been ascertained indeed in some of these rocks by means of microscope analyses. However, some sample population (e.g. *FR, CO)* in which only one diffraction peak was found, include some rock samples in which detrital muscovite turns out to be abundant in thin section. Therefore, another explanation should be found at least for such sample populations, and could be extended to all the other populations. Although Alpine metamorphic effects have been never found in the PCC post-Variscan cover, we cannot exclude that some metamorphic overprint could have been locally produced during the multistage Alpine deformation (RAINITSCH, 1993; LÄUFER, 1994). In such a case, the $d_{33\bar{1},060}$ values of the second muscovite should be related to the pressure conditions of this hypothetical Alpine metamorphic overprint rather than to the crystallization conditions of the old clastic micas.

Figure 4 and table 6 show that the prevailing mica generation (*m* in this table), i.e. the mica population crystallized during the main phase of the Variscan metamorphism, has low $6d_{33\bar{1},060}$ averages, in the range 8.983–8.997 Å. In contrast, the other, subordinate mica population of possible detrital or/and Alpine metamorphic origin (*d* in the table 6) have higher $6d_{33\bar{1},060}$ average values, approximately in the range 9.008–9.022 Å. Figure 5 shows that the average $6d_{33\bar{1},060}$ value of the mica population related to the Variscan metamorphism clearly falls in the low pressure field, while that of the detrital and/or Alpine micas falls in the field of the medium pressure metamorphism.

In order to give unequivocal explanation for the latter micas, systematic $d_{33\bar{1},060}$, K–Ar geochronological and if possible, electron microprobe investigations of white micas belonging to various grain-size fractions are planned from each sample group.

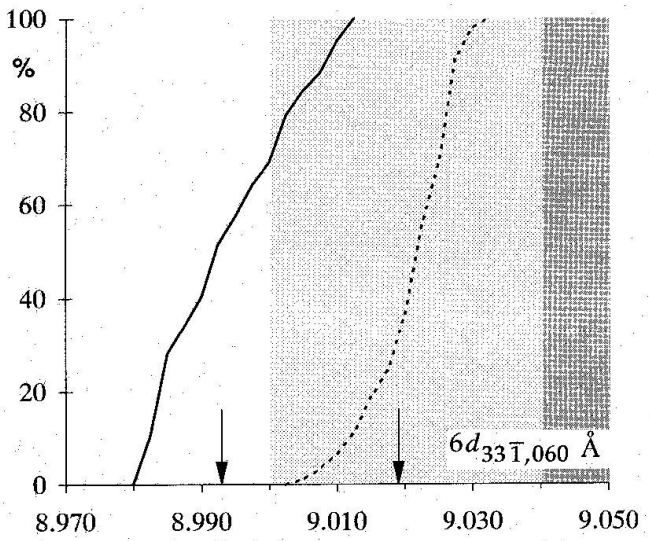


*Fig. 5* Cumulative frequency curves for the whole data set: solid line corresponds to the newly formed micas and the dashed one to detrital or/and Alpine micas (white area = low pressure field; light grey area = medium pressure field; grey area = high pressure field; vertical arrows: average values). The $6d_{33\bar{1},060}$ boundary values between the low, medium and high pressure field are taken from SASSI and GUIDOTTI (1986).

## Concluding remarks

The problem of the boundary location between the Southalpine Metamorphic Basement and the "non-metamorphic" Paleocarnic Chain may be considered as solved by the results of the present paper. This boundary turns out to have a tectonic character. In fact, as shown in figure 6, the IC and coal rank data clearly indicate that the epimetamorphic realm within the Southalpine Basement is confined to the west of Val Bordaglia Line (VBL) and that anchimetamorphic conditions are recorded to the east of it. However, a regular metamorphic gradient is not shown, due to the several tectonic lines and thrust planes which dismember this area in several tectonic units. Anyway, notwithstanding these structural complexities, the above data show that the block to the east of the VBL was located at cooler crustal levels within the thermal Variscan structure, than the western block.

Three further main considerations can be stressed from this work: (i) the extension of the MSB is significantly larger than previously sup-

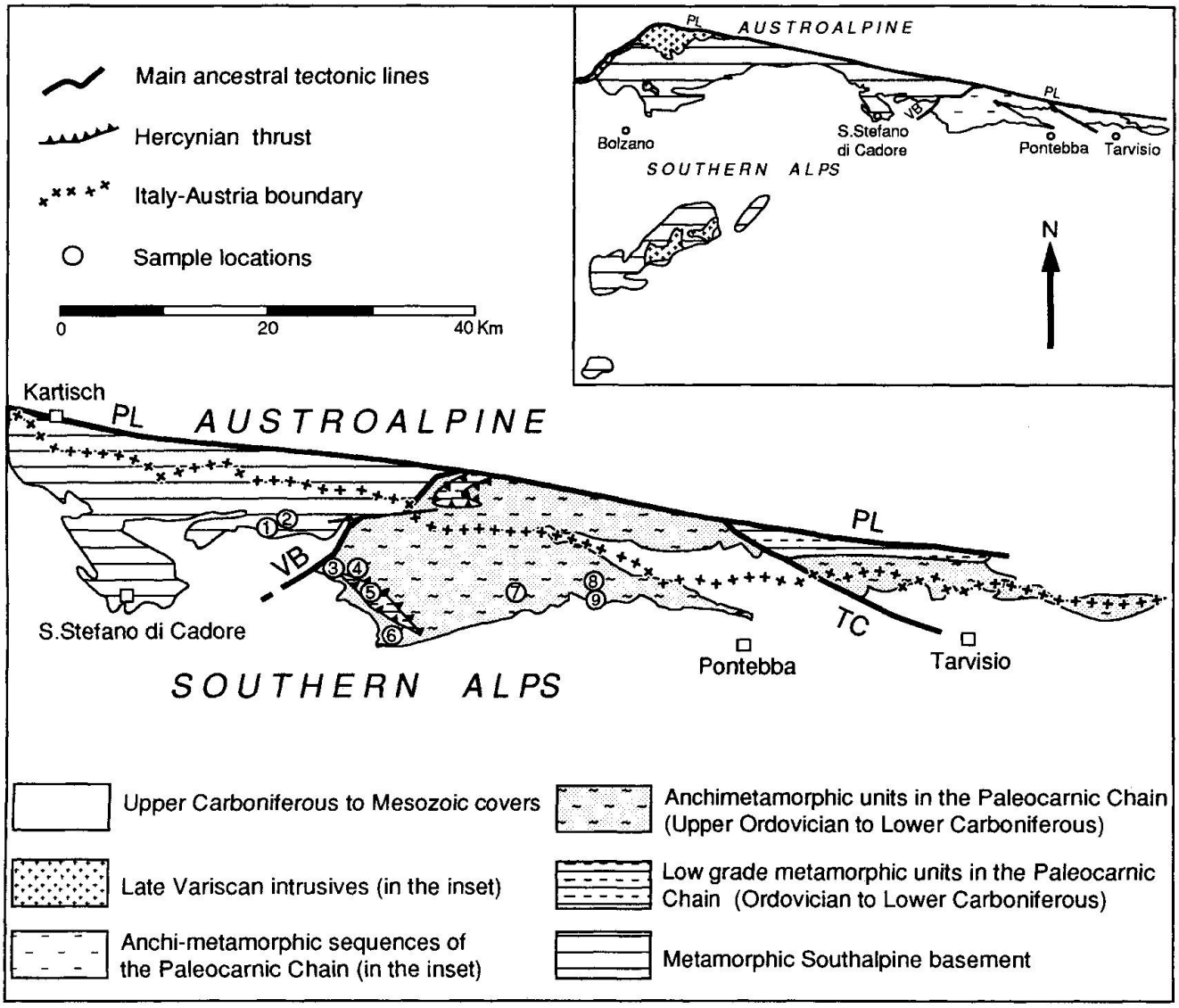


*Fig. 6* New, northeastern boundary of the Metamorphic Southalpine Basement as turns out from the results of the present paper (sample locations as in Fig. 1).

posed; (ii) previously assumed "non-metamorphic" PCC is anchimetamorphic indeed; (iii) it includes tectonic slices of epizonal metamorphics.

As regards the interpretation of these tectonic slices, two alternative hypotheses may be proposed:

a) the $D_2$ folding stage, the effects of which are the only ones which have been detected in this part of the Variscan Chain, could have produced epizonal metamorphism at deep crustal levels, and these epizonal rocks could have been locally brought at shallower levels during the imbricate-slice producing $D_2$ "tectonic stage";

b) these epimetamorphic tectonic slices, which also occur in the adjacent Austrian areas (Garnitzenklamm, Mauthner Alm), could be the result of local deformations which might have affected the cores of south-vergent huge tight folds during $D_2$ tectonic stage.

Whatever the correct interpretation is, the cartographic representation of the MSB and regional distribution of the Variscan metamorphic effects is significantly changed on the base of the results of this paper.

## Acknowledgements

Financial support to RS by the Italian MURST (40 and 60% funds) and C.N.R. (Centro di Studio per la Geodinamica Alpina) are acknowledged. RS also thanks Caterina for her assistance in the field work. PÁ acknowledges financial support by the Hungarian National Research Fund, research program No. T007211/1993–1996 (OTKA, Budapest). Financial support to CV by Italian

MURST (40% fund) is also acknowledged. The text benefited of the helpful suggestions by M. Frey and R.F. Mählmann.

## References

ÁRKAI, P. (1982): Incipient regional metamorphism (on the examples of the Szendró, Uppony and Bükk Mountains, NE-Hungary). C.Sc. Thesis, Budapest (in Hungarian).

ÁRKAI, P., SASSI, R. and ZIRPOLI, G. (1991): On the boundary between the low- and very low-grade southalpine basement in Pustertal: X-ray characterization of muscovite in metapelites between Dobbiaco (Toblach, Italy) and Leiten (Austria) (Eastern Alps). Mem. Sci. Geol., 43, 293–304.

CASSINIS, G., PEROTTI, C.R. and VENTURINI, C. (1993): Examples of Late Hercynian transtensional tectonics in Southern Alps (Italy) (in print).

ESSENE, E.J. (1989): The current status of thermobarometry in metamorphic rocks. In: DALY, J.S., CLIFF, R.A. and YARDLEY, B.W.D. (eds): Evolution of Metamorphic Belts. Geol. Soc. Spec. Publ., 43, 1–44, Oxford.

FREY, M. (1987): Very low grade metamorphism of clastic sedimentary rocks. In: M. FREY (ed.): Low temperature metamorphism. Blackie & Son Ltd, 9–58, Glasgow.

FREY, M. and NIGGLI, E. (1972): Magarite, an important rock-forming mineral in regionally metamorphosed low-grade rocks. Die Naturwissenschaften, 59, 214–215, Berlin.

GUIDOTTI, C.V. and SASSI, F.P. (1976): Muscovite as a petrogenetic indicator mineral in pelitic schists. N. Jb. Miner. Abh., 127, 97–142.

GUIDOTTI, C.V. and SASSI, F.P. (1986): Classification and correlation of metamorphic facies series by means of muscovite b data from low-grade metapelites. N. Jb. Miner. Abh., 153, 363–380.

GUIDOTTI, C.V., MAZZOLI, C., SASSI, F.P. and BLENCOE, G. (1992): Compositional controls on cell dimensions of $2M_1$ muscovite and paragonite. Eur. J. Mineral., 4, 283–297.

KÜBLER, B. (1968): Evaluation quantitative de métamorphisme par la cristallinité de l'illite. Bulletin Centre de Recherches de Pau SNPA, 2, 385–397, Pau.

KÜBLER, B. (1975): Diagenèse – anchimétamorphisme et métamorphisme. Institute national de la recherche scientifique – Pétrole. Québec.

KÜBLER, B. (1990): "Cristallinité" de l'illite et mixed-layers: brève révision. Schweiz. Mineral. Petrogr. Mitt., 70, 89–93.

LÄUFER, A. (1994): Effects of Variscan Orogeny in the Carnic Alps (Austria/Italy). J. Czech Geol. Soc., 39, 64–65.

LÄUFER, A., LOESCHKE, J. and VIANDEN, B. (1993): Die Dimon-Serie der Karnischen Alpen (Italien). Stratigraphie, Petrographie und geodynamische Interpretation. Jb. Geol, B.A., 136, 137–162, Wien.

LEZZERINI, M., SARTORI, F. and TAMPONI, M. (1995): Effects on specimens thickness on illite "crystallinity" measurements. Eur. J. Mineral., 7, 4 (in press).

MANZONI, M. (1970): Paleomagnetic data of Middle and Upper Triassic age from the Dolomites (Eastern Alps, Italy). Tectonophysics, 10, 411–424.

MANZONI, M., VENTURINI, C. and VIGLIOTTI, L. (1989): Paleomagnetism of Upper Carboniferous limestones from the Carnic Alps. Tectonophysics, 165, 73–80.

MENEGAZZI, R., PILI, M. and VENTURINI, C. (1991): Preliminary data and hypothesis about the very low grade metamorphic Hercynian sequence of the western Paleocarnic chain. Giornale di Geologia, 53, 139–150.

METAMORPHIC MAP OF THE ALPS (1973): scale 1 : 1.000.000. IUGS Subcommission for the cartography of the Metamorphic Belts of the World. Leiden/UNESCO, Paris. Movton & Co. N.V. The Hague.

PADAN, A., KISCH, H.J. and SHAGAM, R. (1982): Use of the lattice parameter b of dioctahedral illite/muscovite for the characterization of P/T gradients of incipient metamorphism. Contr. Mineral. Petrol., 79, 85–95.

RANITSCH, G. (1993): Zur Wärmegeschichte der Karnischen Alpen (Österreich). Unpubl. Ph.D. thesis, Univ. of Graz, 1–173, Graz.

RIEDER, M., GUIDOTTI, C.V., SASSI, F.P. and WEISS, Z. (1992): Muscovites: $d_{060}$ versus $d_{33\bar{1},060}$ spacing: its use for geobarometric purposes. Eur. J. Mineral., 4, 843–845.

SASSI, F.P. (1972): The petrological and geological significance of the b values of potassic white micas in low-grade metamorphic rocks. An application to the Eastern Alps. Tschermaks Miner. Petrogr. Mitt., 18, 105–113, Wien.

SASSI, F.P. and SCOLARI, A. (1974): The *b* value of the potassic white micas as a barometric indicator in low-grade metamorphism of pelitic schists. Contr. Mineral. Petrol., 45, 143–152.

SASSI, F.P., NEUBAUER, F., MAZZOLI, C., SASSI, R., SPIESS, R. and ZIRPOLI, G. (1994): A tentative comparison of the Paleozoic evolution of the Austroalpine and Southalpine quartzphyllites in the Eastern Alps. Per. Min., 63, 1/3, 35–52.

SELLI, R. (1963): Schema geologico delle Alpi Carniche e Giulie Occidentali. Giorn. Geol., 2, 30, 1–136, Bologna.

SPALLETTA, C., VAI, G.B. and VENTURINI, C. (1982): La Catena Paleocarnica. In: CASTELLARIN, A. and VAI, G.B. (eds): Guida alla geologia del Sudalpino centro-orientale. Guida Geol. Reg. S.G.I., 281–292, Bologna.

STRUCTURAL MODEL OF ITALY AND GRAVITY MAP (1990): Scale 1:500.000. CNR. Selca Firenze 1990.

VAI, G.B. (1976): Stratigrafia e paleogeografia ercinica delle Alpi. Mem. Soc. Geol. It., 13 (1), 7–37.

VAI, G.B. (1979): Una palinspastica permiana della Catena Paleocarnica. Rend. Soc. Geol. It., 1, 29–30.

VAI, G.B., BORIANI, A., RIVALENTI, G. and SASSI, F.P. (1984): Catena ercinica e Paleozoico nelle Alpi Meridionali. In: Cento anni di geologia italiana. Vol. giub. 1° Centenario S.G.I., 133–154, Roma.

VENTURINI, C. (1990): Geologia delle Alpi Carniche centro orientali. Museo Friulano di Storia Naturale, Pubbl. 36, 1–222, Udine.

VENTURINI, C. (1991): Introduction to the geology of the Pramollo Basin (Carnic Alps) and its surroundings. In: VENTURINI, C. (ed.): Workshop Proceedings on Tectonics and Stratigraphy of the Pramollo Basin (Carnic Alps). Giorn. Geol., 3, 53(1), 13–47.

VENTURINI, C. and DELZOTTO, S. (1992): Evoluzione deformativa delle Alpi Carniche centro occidentali: paleotettonica e tettonica neoalpina. Studi Geol. Camerti, Vol. Spec. (1992/2), CROP 1-1A, 261–270.

Manuscript received February 15, 1995; revision accepted June 15, 1995.